

---

# Bosonic Random Walk Networks for Graph Learning

---

**Shiv Shankar**

College of Information and Computer Science  
University of Massachusetts  
sshankar@cs.umass.edu

**Don Towsley**

College of Information and Computer Science  
University of Massachusetts  
towsley@cs.umass.edu

## Abstract

The development of Graph Neural Networks (GNNs) has led to great progress in machine learning on graph-structured data. These networks operate via diffusing information across the graph nodes while capturing the structure of the graph. Recently there has also seen tremendous progress in quantum computing techniques. In this work, we explore applications of multi-particle quantum walks on diffusing information across graphs. Our model is based on learning the operators that govern the dynamics of quantum random walkers on graphs. We demonstrate the effectiveness of our method on classification and regression tasks.

## 1 Introduction

The current era of ubiquitous connectivity has provided researchers with ever-increasing troves of data. Most of such ‘real-world’ data have an underlying graphical structure that can be utilized to build better models and derive greater insights. Such graphical structures are not limited to the web, social networks, or other network systems. Graph-structured problems are also common in many scientific fields such as immunology (Crossman, 2020), chemical analysis (John et al., 2019) and bio-chemistry (Bonetta and Valentino, 2019).

Current machine learning approaches for analyzing structured data can be broadly categorized into neural approaches and classical approaches. Classical approaches rely on comparing graphs directly via walks (Dobson and Doig, 2003; Callut et al., 2008) or by utilizing other similarity notions (Kondor et al. (2009); Kondor and Borgwardt (2008)). A related technique is to use graph kernels (Vishwanathan et al., 2010; Gärtner et al., 2003) to define a notion of similarity between graphs. There have been some recent works (Bai et al., 2017a) that try to define similarity using quantum walks.

The last decade also saw great progress in machine learning via the development of deep-learning techniques. Some of these works also focused on applying neural networks to graph-structured data (Defferrard et al., 2016; Duvenaud et al., 2015) Duvenaud et al. (2015) present a method for differentiable fingerprinting where the hashing functions are replaced by neural networks. Defferrard et al. (2016) extend the convolution operator to graphs using graph Laplacians. Kipf and Welling (2017) use the same technique for semi-supervised learning on graphs. Atwood and Towsley (2016) also, extend convolutions to graphs via graph diffusions. Building upon these works and the ideas of Bai et al. (2017a), Dernbach et al. (2019) incorporate quantum walks into a neural network.

In this paper, we explore the application of some quantum computing techniques in graph learning. We first summarize some basic principles relevant to our approaches in Section 2. Next, we present a graph learning method that is inspired by these quantum ideas. Our approach is a hybrid one that a) uses quantum walks to learn diffusions and b) utilizes the diffusions in a classical way. Finally, we present the results of our experiments.

## 2 Preliminaries

### 2.1 Bosonic Quantum Mechanics

Photonic circuits are a prime candidate for both near-term and future quantum devices. Photons are a type of boson that lead to interesting statistical and physical phenomena. Hence understanding some key aspects of bosonic quantum systems is important when considering possibly physical realization of some quantum algorithms.

An important characteristic of bosons is that two bosons of the same type are indistinguishable; and this has interesting consequences. Let us denote system state by  $|\psi(x_1, x_2)\rangle$  where  $\psi$  is some function and  $x_1, x_2$  are generalized coordinates (eg position, state etc) of the two particles. The exchange operator  $E$  is then defined by the following action

$$E |\psi(x_1, x_2)\rangle = |\psi(x_2, x_1)\rangle$$

Informally the exchange operator swaps the coordinates/states of the individual particles in the combined system. The requirement of indistinguishability is the invariance of a multi-particle system to the exchange operator. Imagine a system having binary states  $|0\rangle, |1\rangle$  and two particles that can occupy those states. The standard computational decomposition for the Hilbert space of such a system has 4 basis viz.  $|00\rangle, |11\rangle, |01\rangle, |10\rangle$ ; corresponding to the states of each of the two particles. One can imagine that the system is described by the state  $|01\rangle$ . However, indistinguishability means we can permute the labels of the particles and the system is equally be described by  $|10\rangle$ . Note that this along with the superposition principle implies that any superposition of the these states is an equally valid description of the state. This leads to the following principle:

**Symmetrization Postulate for Bosons** In a system of indistinguishable bosons, the only possible states of the system are ones that are symmetric with respect to permutations of the labels of those particles.

The Symmetrization Postulate restricts the Hilbert space of the system to lie in the completely symmetric subspace. In the specific case considered above the Hilbert space of this system is spanned by 3 states instead of the usual 4. Furthermore the postulate implies that result of any measurement of a state must project the state into the symmetric indistinguishable subspace.

#### 2.1.1 Fock space

Indistinguishability also implies that only the total number of bosons in a given state has any meaning. This makes it convenient to use an alternate basis for describing the Hilbert space of the system known as the Fock basis. It is a construction for the state space of a variable or unknown number of identical particles from the Hilbert space of a single particle. For bosons, the  $n$ -particle states are elements in the symmetric product of  $n$  uni-particle Hilbert spaces. For more details of the Fock space notation refer to the Appendix A

**Creation and Annihilation Operators** Operations in the Fock space bases are written as unitary matrices of creation and annihilation operators. As its name suggests the creation (or raising) operator (denoted commonly by  $a$ ) adds a particle to the state it operates on, while the annihilation (lowering) operator ( $a^\dagger$ ) does the opposite.

### 2.2 Quantum Walks

A classical walk on a graph  $G = (V, E)$  can be described as follows. At any given timestep  $t$  the walker resides at one of the nodes of the graph say  $u$ . Each node has an associated multiheaded coin with each head corresponding to an incident edge. Equivalently there is a multinomial distribution over the edges incident on the node. The walker then draws an edge according to the distribution (say  $e = (u, v)$ ). The walker then moves to the node  $v$  which is connected to  $e$ .

Quantum walks are the quantum extension of a classical random walk. A classical walk involves a walker moving around on a graph and at any point in time its position is given by a probability

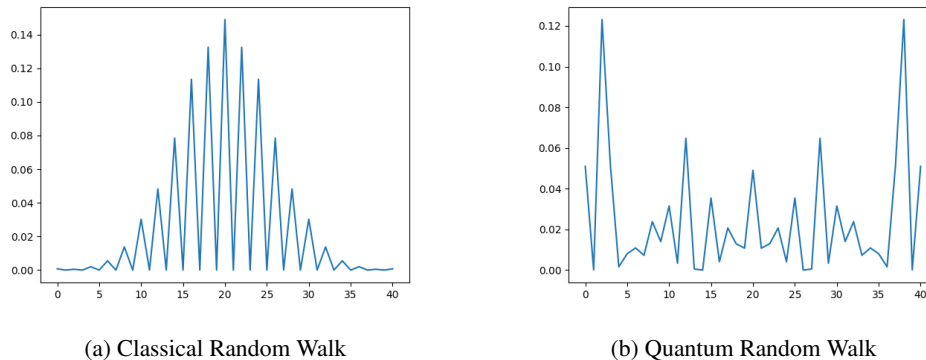


Figure 1: Comparing classical and quantum walk

distribution. A quantum walk is similar, however instead of a random process the walkers movement is governed by a sequence of unitary operations. Unlike a classical walk where the walker can only be at a node, the quantum walker can be in a superposition over all nodes in the graph.

We follow the approach of [Kendon \(2011\)](#) in describing quantum walks. A quantum walk involves two Hilbert spaces: the position space  $\mathcal{H}_v$  corresponding to nodes of the graph; and a coin space  $\mathcal{H}_c$ . To preserve unitarity the size of the coin space is fixed across all nodes. This can be achieved by taking the maximum degree of the nodes as the size of the space. The quantum walker’s state is determined by the combined space of position and coin combinations. Instead of a coin toss, we now have a unitary operator  $C$  (called the coin operator) on the coin space describing the evolution of the coin-part of the walkers state. We also have a shift operator  $S$ . The shift operator acts as a conditional gate: depending on the coin state it swaps the coefficients of the corresponding positions. The evolution of the entire system is given by the unitary operator  $U = S(I \otimes C)$

This kind of evolution produces a behavior completely unlike that of a classical walk. The superposition of states allows walker trajectories to interfere: something that cannot happen classically. This interference can lead to a faster spreading of the walker’s final position distribution. The clear effect of this can be seen in [Figure 1](#). These figures show the result of simulating a classical and quantum walk on a 1-d lattice for 30 steps. The final state distribution of classical walk is shown in [Figure 1a](#). It is clearly centered around its starting point and has a exponentially falling tail as one moves further from the start.

The quantum walk however ([Figure 1b](#)) shows a very different picture. While the mean of the walk is still at the starting point, the distribution modes are peaks far away from the start. Such behavior allows a quantum random walker to have significantly better exploration. Inspiring from this insight [Dernbach et al. \(2018\)](#) proposed a version of diffusion networks based upon quantum walks. They demonstrated that using probability distribution of quantum walkers allows for far better exploration and incorporation of graph structure as compared to classical approaches.

### 3 Bosonic Walks Networks

A natural question with respect to random walk based graph networks is whether incorporation of multiple walkers can lead to a different outcome. While multiple non-interacting classical walkers have no extra power compared to a single classical walker, the answer is different for quantum walkers ([Chandrashekar and Busch, 2012](#)). A key reason for this is the symmetrization postulate referred to earlier.

#### 3.1 Bosonic Quantum Walks

Bosonic walks can a) have unintuitive non-local correlations across walker states and b) allow for dynamics not accessible for distinguishable particles. As such even limited bosonic walks can have surprising power. For example [Gamble et al. \(2010\)](#) demonstrate that there are classes of non-isomorphic graphs that can be distinguished by the node distribution of multi-particle walks but

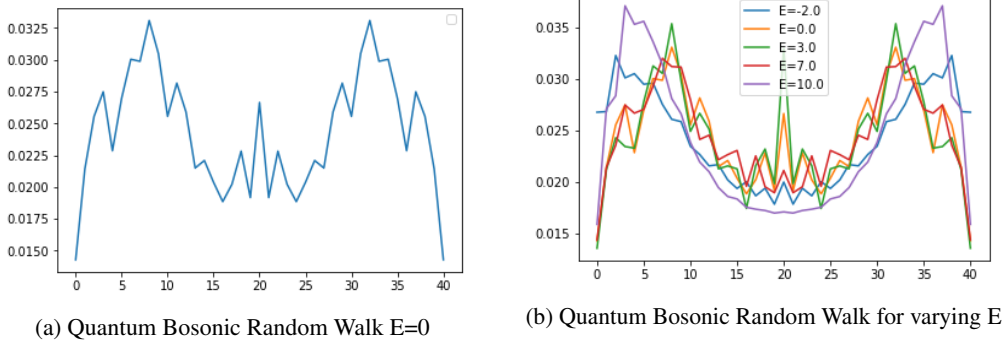


Figure 2: Comparing quantum walks with difference interaction energy  $U$

not by the node distribution of a single particle quantum walk. More recently [Lahini et al. \(2018\)](#) have proposed a scheme for implementing high-fidelity quantum gates using a multiple bosonic quantum walkers.

We focus on a setting with multiple bosonic particles executing quantum walks on a graph. The Hilbert space of these walkers allow significantly more trajectories of the walker by allowing entangled coins and other complexities. The evolution of the walkers state in the Fock space basis is driven by the Hamiltonian  $H$  given by

$$H = A_{ij}c_i^\dagger c_j + E c_i c_i^\dagger (c_i c_i^\dagger - 1)$$

$A$  is the adjacency matrix of the graph and  $c_i, c_i^\dagger$  are creation and annihilation operators associated with node  $i$ .  $E c_i c_i^\dagger (c_i c_i^\dagger - 1)$  is a term which describes the interaction between the walkers and  $E$  is the interaction strength. Note that when the particles are in different nodes, the interaction term has no effect.

Similar to earlier results, we compute the probability of observing a walker across different nodes on a 1-D lattice after 30 steps in the case when  $E = 0$ . This is plotted in [Figure 2a](#), where we can notice easy differences between this plot and the plot of the single particle quantum walk discussed earlier. Next we plot the probability of observing a walker for different values of  $E$  in [Figure 2b](#). Note the probability distribution changes significantly as the interaction strength changes.

### 3.2 Bosonic Quantum Walk Neural Networks

A Bosonic Quantum Walker Network (QWB) is the natural extension of the [Dernbach et al. \(2018\)](#) model using bosonic quantum walkers. For our description below, we will follow a similar presentation. The key idea behind a quantum walk neural network is to use the walker’s distribution over the nodes of a graph to construct a diffusion matrix, which is then utilized to aggregate information from the nodes. At each time step, we simulate the dynamics of the walker using the coin operator,  $C$ , to modify the spin state of the walkers  $\psi$  according to  $C(t)\psi_t \rightarrow \psi_{t+1}$ . The coin operator need not be static and can depend on both time and node features. This is followed by the shift operator, which moves the walker to a neighbouring node depending upon the walker spin state. The walker dynamics induces a probability distribution of the walker over the graph (written as a probability matrix  $P$ ). Next, this matrix  $P$  is used to diffuse the node level features across the graph:  $\hat{X} = PX$ . These diffused features are the output of a single quantum diffusion layer. These features can then be used either as input for a second diffusion layer; or for final prediction. All of these operations are differentiable, and hence we can use backpropagation to compute the gradient of the loss with respect to all the model parameters (especially parameters of the coin matrix) .

Note that the description till here is independent of how the walkers behave. In fact, walkers can behave completely classically, in which case the behaviour is identical to the Diffusion Convolution model of [Atwood and Towsley \(2016\)](#). For a quantum walk network, the walk dynamics are governed by quantum evolution. The induced probability matrix is the one determined by the measurement of

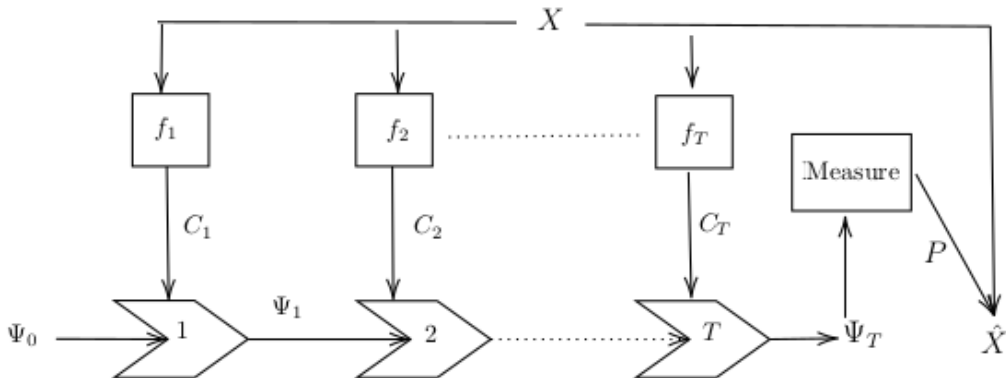


Figure 3: Quantum Walk Neural Network Schematic: The feature matrix  $X$  is used to produce the coin operators  $C_i$  used in each step  $i$ . The superposition  $\psi$  evolves after each step. The final layer diffuses  $X$  using measured probabilities  $P$  to compute  $\hat{X}$

the walker’s node-state. We compute  $P$  induced by a bosonic multi-particle quantum walk on the graph in the bosonic quantum walk model. This can be achieved via evolving single-particle walkers and then performing a projection into the indistinguishable space by performing repeating sums over identical labels. More details are available in Appendix C

Since a  $k$ -particle quantum walk naturally produces a symmetric superposition over  $k$ -tuples of nodes, we can, in principle, extend  $P$  from a distribution over nodes to a distribution over node pairs or even higher orders. In our experiments, however, we do not use such higher-order features. Instead, we compute  $P$  from the probability of observing *a single* boson at the given nodes.

## 4 Experiments

**Datasets** We experiment with commonly used graph datasets: QM7, which is a regression task and MUTAG, NCI1, and Enzymes (which are classification problems). MUTAG [Debnath et al. \(1991\)](#) is a dataset of 188 mutagenic aromatic and heteroaromatic nitro compounds that are classified as either mutagenic or not. NCI1 [Wale and Karypis \(2006\)](#) consists of 4110 graphs representing two sets of chemical compounds screened for activity against non-small cell lung cancer. For both these datasets, each graph represents a molecule, with nodes representing atoms and edges representing bonds between atoms. Each node has an associated label that corresponds to its atomic number. Enzymes [Borgwardt et al. \(2005\)](#) is a dataset of 600 molecules where the task is to classify each enzyme into one of six classes. The QM7 dataset [Rupp et al. \(2012\)](#); [Blum and Reymond \(2009\)](#) is a collection of 7165 molecules, each containing up to 23 atoms. The goal of the task is to predict the atomization energy of each molecule.

**Experimental Details** We include as baselines two classical methods (DCNN, GCN). DCNN refers to the diffusion convolutional network of [Atwood and Towsley \(2016\)](#), while GCN is the graph convolution architecture of [Kipf and Welling \(2017\)](#). QWNN is the quantum walk based model presented in [Dernbach et al. \(2019\)](#). QWB2 is our two-particle bosonic extension of the QWNN model. The metric used for classification tasks (NCI, MUTAG, Enzymes) is accuracy (so higher the better) while the one used for QM7 is mean prediction error (so lower the better).

Classical simulation of quantum walks has poor scaling properties. Simulating a  $k$ -particle quantum walk scales exponentially in  $k$ . As such in our experiments we restricted ourselves to graphs of size less than 70 and had to reduce sizes of feature embeddings. Furthermore to keep comparison fair in terms of feature size between classical and quantum models, we applied the same restriction to the classical models as well. For more details on the parameters used refer to Appendix D.

**Results** Table 1a reports the classification performance of different models. We see that QWB2 outperforms other models, especially on Enzymes where the gain is substantial. QWB2 also outper-

forms QWNN and other classic approaches on MUTAG and NCI datasets. Regression results on QM7 are presented in Table 1b. The basic trend of QWB2 outperforming other approaches remains, though the performance differences are comparatively smaller. Overall QWB2 seems to outperform all other models including its single-walker counterpart QWNN.

Model	Enzymes	MUTAG	NCI
GCN	31.4	87.4	69.6
DCNN	27.9	89.1	69.1
QWNN	33.6	88.4	73.6
QWB2	<b>40.2</b>	<b>90.0</b>	<b>76.7</b>

(a) Classification tasks

Model	MSE	MAE
GCN	17.5	12.4
DCNN	11.9	8.6
QWNN	10.9	8.4
QWB2	<b>9.2</b>	<b>7.9</b>

(b) Atomization energy prediction on QM7

Table 1: Results of different models on graph classification and regression tasks

## 5 Related Work

**Graph Neural Networks** Early graph neural networks (GNN) (Gori et al., 2005; Scarselli et al., 2008) used recursive architectures to encode graphs into finite-dimensional vectors. Since then has been tremendous progress in learning representations of graphs. Convolutional neural networks (Bruna et al., 2013; Defferrard et al., 2016; Kipf and Welling, 2017) borrow ideas from graph Laplacians (Cvetkovic et al., 1998) for processing graphs signals. Atwood and Towsley (2016), on the other hand, proposed a spatial approach relying on random walks. Gilmer et al. (2017) proposed a general approach for learning on graphs via message passing between nodes of the graphs. All the other mentioned works can be interpreted as a restricted version of that approach.

**Quantum Models** There is a rich literature exploring quantum walks beginning with works of Ambainis et al. (2001) and Aharonov et al. (2001). A generalization of discrete walks for an arbitrary number of walkers was studied by Rohde et al. (2011). Subsequently, multiple works have developed graph kernels based on the quantum walks (Rossi et al., 2013; Bai et al., 2013, 2017b). Quantum walks have also been shown to provide a model for universal computation Childs (2009). They have been explored for algorithmic applications Childs and Eisenberg (2003); Qiang et al. (2012) and quantum simulation Berry et al. (2005). While there have been multiple proposals of quantum neural networks over the years Gupta and Zia (2001); Biamonte et al. (2017); there has been not much work done on quantum learning techniques for graphs. Our work derives from the recent work of Dernbach et al. (2018), which proposed a quantum version of graph diffusion networks.

## 6 Conclusion

Quantum devices based on bosons are a prime candidate for future quantum. As such techniques which can directly leverage the behavior of bosons are important to explore. In this work we have tried to incorporate multi-particle bosonic walks on graphs. Unlike simple QWNN, this approach allows for learning significantly more powerful and complex graph diffusions. This benefit is clear across both regression and classification tasks. A future research direction would be to find ways to constrain the multiple walkers such that the simulation becomes more feasible.

## References

- D. Aharonov, A. Ambainis, J. Kempe, and U. Vazirani. Quantum walks on graphs. In *Proceedings of the thirty-third annual ACM symposium on Theory of computing*, pages 50–59, 2001.
- A. Ambainis, E. Bach, A. Nayak, A. Vishwanath, and J. Watrous. One-dimensional quantum walks. In *Proceedings of the thirty-third annual ACM symposium on Theory of computing*, pages 37–49, 2001.
- J. Atwood and D. F. Towsley. Diffusion-convolutional neural networks. In *NIPS*, 2016.

- L. Bai, E. R. Hancock, A. Torsello, and L. Rossi. A quantum jensen-shannon graph kernel using the continuous-time quantum walk. In *International Workshop on Graph-Based Representations in Pattern Recognition*, pages 121–131. Springer, 2013.
- L. Bai, L. Rossi, L. Cui, Z. Zhang, P. Ren, X. Bai, and E. Hancock. Quantum kernels for unattributed graphs using discrete-time quantum walks. *Pattern Recognition Letters*, 87, 02 2017a.
- L. Bai, L. Rossi, L. Cui, Z. Zhang, P. Ren, X. Bai, and E. Hancock. Quantum kernels for unattributed graphs using discrete-time quantum walks. *Pattern Recognition Letters*, 87:96–103, 2017b.
- D. Berry, G. Ahokas, R. Cleve, and B. Sanders. Efficient quantum algorithms for simulating sparse hamiltonians. *Commun. Math. Phys.*, 270, 09 2005. doi: 10.1007/s00220-006-0150-x.
- J. Biamonte, P. Wittek, N. Pancotti, P. Rebentrost, N. Wiebe, and S. Lloyd. Quantum machine learning. *Nature*, 549(7671):195–202, 2017.
- L. C. Blum and J.-L. Reymond. 970 million druglike small molecules for virtual screening in the chemical universe database gdb-13. *Journal of the American Chemical Society*, 131(25): 8732–8733, 2009.
- R. Bonetta and G. Valentino. Machine learning techniques for protein function prediction. *Proteins: Structure, Function, and Bioinformatics*, 88, 10 2019.
- K. M. Borgwardt, C. S. Ong, S. Schönauer, S. Vishwanathan, A. J. Smola, and H.-P. Kriegel. Protein function prediction via graph kernels. *Bioinformatics*, 21(suppl\_1):i47–i56, 2005.
- J. Bruna, W. Zaremba, A. Szlam, and Y. LeCun. Spectral networks and locally connected networks on graphs. *arXiv preprint arXiv:1312.6203*, 2013.
- J. Callut, K. Francois, M. Saerens, and P. Dupont. Classification in graphs using discriminative random walks. In *International Workshop on Mining and Learning with Graphs*, 07 2008.
- C. M. Chandrashekar and T. Busch. Quantum walk on distinguishable non-interacting many-particles and indistinguishable two-particle. *Quantum Information Processing*, 11(5):1287–1299, Mar 2012.
- A. M. Childs. Universal computation by quantum walk. *Phys. Rev. Lett.*, 102:180501, 2009.
- A. M. Childs and J. M. Eisenberg. Quantum algorithms for subset finding. *Quantum Information and Computation*, 5:593–604, 2003.
- Contributors. Fock state — Wikipedia, the free encyclopedia. URL [https://en.wikipedia.org/wiki/Fock\\_space](https://en.wikipedia.org/wiki/Fock_space). [Online; accessed 2-May-2020].
- L. C. Crossman. Leveraging deep learning to simulate coronavirus spike proteins has the potential to predict future zoonotic sequences. *bioRxiv*, 2020.
- D. Cvetkovic, M. Doob, and H. Sachs. Spectra of graphs: Theory and applications, 3rd rev. enl. ed, 1998.
- A. K. Debnath, R. L. Lopez de Compadre, G. Debnath, A. J. Shusterman, and C. Hansch. Structure-activity relationship of mutagenic aromatic and heteroaromatic nitro compounds. correlation with molecular orbital energies and hydrophobicity. *Journal of Medicinal Chemistry*, 34(2):786–797, 1991.
- M. Defferrard, X. Bresson, and P. Vandergheynst. Convolutional neural networks on graphs with fast localized spectral filtering. In *NIPS*, 2016.
- S. Dernbach, A. Mohseni-Kabir, S. Pal, D. Towsley, and M. Gepner. Quantum walk inspired neural networks for graph-structured data. *arXiv: Quantum Physics*, 2018.
- S. Dernbach, A. Mohseni-Kabir, S. Pal, M. Gepner, and D. Towsley. Quantum walk neural networks with feature dependent coins. *Applied Network Science*, 4:76, 09 2019. doi: 10.1007/s41109-019-0188-2.
- P. Dobson and A. Doig. Distinguishing enzyme structures from non-enzymes without alignments. *Journal of molecular biology*, 330:771–83, 08 2003.
- D. K. Duvenaud, D. Maclaurin, J. Iparraguirre, R. Bombarell, T. Hirzel, A. Aspuru-Guzik, and R. P. Adams. Convolutional networks on graphs for learning molecular fingerprints. In *Advances in Neural Information Processing Systems 28*, pages 2224–2232. 2015.
- J. K. Gamble, M. Friesen, D. Zhou, R. Joynt, and S. N. Coppersmith. Two-particle quantum walks applied to the graph isomorphism problem, 2010.

- J. Gilmer, S. S. Schoenholz, P. F. Riley, O. Vinyals, and G. E. Dahl. Neural message passing for quantum chemistry. *arXiv preprint arXiv:1704.01212*, 2017.
- M. Gori, G. Monfardini, and F. Scarselli. A new model for learning in graph domains. In *Proceedings. 2005 IEEE International Joint Conference on Neural Networks, 2005.*, volume 2, pages 729–734. IEEE, 2005.
- S. Gupta and R. Zia. Quantum neural networks. *Journal of Computer and System Sciences*, 63(3): 355–383, 2001.
- T. Gärtner, P. Flach, and S. Wrobel. On graph kernels: Hardness results and efficient alternatives. volume 129-143, pages 129–143, 01 2003.
- P. S. John, Y. Guan, Y. Kim, S. Kim, and R. Paton. Prediction of Homolytic Bond Dissociation Enthalpies for Organic Molecules at near Chemical Accuracy with Sub-Second Computational Cost. 11 2019.
- V. Kendon. Quantum walks on general graphs. *International Journal of Quantum Information*, 04, 11 2011.
- T. Kipf and M. Welling. Semi-supervised classification with graph convolutional networks. In *ICLR*, 2017.
- R. Kondor and K. M. Borgwardt. The skew spectrum of graphs. In *Proceedings of the 25th International Conference on Machine Learning, ICML '08*, page 496–503, 2008.
- R. Kondor, N. Shervashidze, and K. Borgwardt. The graphlet spectrum. volume 382, page 67, 01 2009. doi: 10.1145/1553374.1553443.
- Y. Lahini, G. R. Steinbrecher, A. D. Bookatz, and D. Englund. Quantum logic using correlated one-dimensional quantum walks. *npj Quantum Information*, 4(1), 2018. ISSN 2056-6387.
- X. Qiang, X. Yang, J. Wu, and X. Zhu. 45(4):045305, 2012.
- L. Rigovacca and C. Di Franco. Two-walker discrete-time quantum walks on the line with percolation. *Scientific Reports*, 6(1), Feb 2016.
- P. P. Rohde, A. Schreiber, M. Štefaňák, I. Jex, and C. Silberhorn. Multi-walker discrete time quantum walks on arbitrary graphs, their properties and their photonic implementation. *New Journal of Physics*, 13(1):013001, 2011.
- L. Rossi, A. Torsello, and E. R. Hancock. A continuous-time quantum walk kernel for unattributed graphs. In *International Workshop on Graph-Based Representations in Pattern Recognition*, pages 101–110. Springer, 2013.
- M. Rupp, A. Tkatchenko, K.-R. Müller, and O. A. von Lilienfeld. Fast and accurate modeling of molecular atomization energies with machine learning. *Phys. Rev. Lett.*, 108:058301, 2012.
- F. Scarselli, M. Gori, A. C. Tsoi, M. Hagenbuchner, and G. Monfardini. The graph neural network model. *IEEE Transactions on Neural Networks*, 20(1):61–80, 2008.
- S. Vishwanathan, N. N. Schraudolph, R. Kondor, and K. M. Borgwardt. Graph kernels. *Journal of Machine Learning Research*, 11(40):1201–1242, 2010.
- N. Wale and G. Karypis. Comparison of descriptor spaces for chemical compound retrieval and classification. In *Sixth International Conference on Data Mining (ICDM-06)*. IEEE, 2006.



## A Fock Space

Fock basis is a construction for the state space of a variable or unknown number of identical particles from the Hilbert space of a single particle. If the identical particles are bosons, the  $n$ -particle states are vectors in the symmetric tensor product of  $n$  single-particle Hilbert spaces (Contributors). In this section we provide a basic introduction to Fock spaces, and the corresponding creation and annihilation operators.

Consider a system which can accommodate particles in  $M$  different states. Let  $B = k_i i \in [0, 1, \dots, M]$  be an orthonormal basis of states in the one-particle Hilbert space. For electronic states in an atom such as the one shown in Figure 4 these can correspond to the ground state shell, the first excited state or higher states.

A Fock state is then defined as the state such that for each  $i$ , the state is an eigenstate of the particle number operator  $\widehat{N}_{k_i}$  corresponding to the  $i$ -th elementary state  $k_i$ . The Fock bases of the state space of the system is then depicted by

$$|n_0, n_1, n_2 \dots n_M\rangle$$

where  $n_i$  denotes the number of particles in the state  $i$ . For the system in 4 this refers to the number of electrons in different shells around the atom. Informally, the Fock bases is a counting basis i.e the bases of zero particle states, one particle states, two particle states, and so on

**Creation and Annihilation Operators** For the state defined earlier the annihilation/creation operators are indexed by the state  $i = 1 \dots M$  and operate as follows:

$$\begin{aligned} a_i^\dagger |n_0, n_1, \dots, n_i, \dots, n_M\rangle &= n_i |n_0, n_1, \dots, n_i - 1, \dots, n_M\rangle \\ a_i |n_0, n_1, \dots, n_i, \dots, n_M\rangle &= n_i |n_0, n_1, \dots, n_i + 1, \dots, n_M\rangle \end{aligned}$$

## B Bosonic Walkers Example

Consider a pair of particles executing a quantum walk on a 1D grid. The coin space of walkers then has two states  $|\uparrow\rangle$  and  $|\downarrow\rangle$ . We assume that the shift operators act in a way such that a walker whose coin is up moves right, and a walker whose coin is down moves left.

Let the current state of the walkers after the action of the coin operator be:

$$|1, -1\rangle \otimes |\uparrow\downarrow\rangle$$

It represents the first walker at position 1 with its coin state being up, while the second walker at position -1 with its coin state being down. From this state, the first particle can only move right and the second can only move left.

However if the particles are boson, then the aforementioned state does not exist in the Hilbert space of the system (as it is not symmetric with respect to the exchange operation). Instead the pair of bosonic walkers will be in a state

$$\frac{1}{\sqrt{2}}(|1, -1\rangle \otimes |\uparrow\downarrow\rangle + |-1, 1\rangle \otimes |\downarrow\uparrow\rangle)$$

From this state the first particle can move both left and right, a motion which is not possible for a non-bosonic walker. Note this was enforced by the symmetrization postulate. Such "nonlocal" correlations across non-interacting particle states is not possible in non-bosonic particles (or in classical case) and is a truly quantum phenomenon.

## C Bosonic Walker Simulation

We implement the simulation of quantum walkers as described in [Gamble et al. \(2010\)](#); [Rigovacca and Di Franco \(2016\)](#). For simplicity, we shall limit the exposition to involve only 2 particles. The generalization to multiple walkers is straightforward.

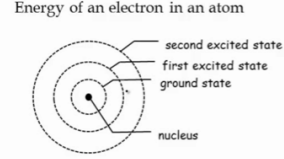


Figure 4: Configuration Space of an Atom

A joint two boson state can be obtained from two single-particle states  $|\psi_1\rangle, |\psi_2\rangle$  with the following symmetrization operation:

$$|\text{Sym}(\psi_1, \psi_2)\rangle = \frac{|\psi_1\rangle \otimes |\psi_2\rangle + |\psi_2\rangle \otimes |\psi_1\rangle}{\sqrt{2(1 + |\langle\psi_1|\psi_2\rangle|^2)}}$$

One should note that the aforementioned symmetrized form cannot represent all the possible states in the symmetric Hilbert space of two bosonic walkers. For example, in walks on a chain, the following state is a physically allowed one:

$$|\psi\rangle = \frac{|ij\rangle + |ji\rangle}{\sqrt{2}} \otimes \frac{|\uparrow\downarrow\rangle + |\downarrow\uparrow\rangle}{\sqrt{2}}$$

where  $i, j$  are indices of nodes in the chain, while  $\downarrow, \uparrow$  represent the coin states. However, we shall limit ourselves to the states expressible in the aforementioned symmetrized form in this work.

Finally, during the measurement stage also, one needs to take into account the symmetrization requirement. This is done by considering a measurement involving the following projector operation::

$$\begin{aligned} \Pi_{ij} &= \frac{1}{2}(|ij\rangle\langle ij| + |ji\rangle\langle ji|) \\ Pr(\psi_t)[i, j] &= \text{Tr}[\Pi_{ij}U_t|\psi_0\rangle\langle\psi_0|U_t^\dagger] \end{aligned}$$

## D Hyperparameter Details

**Classification** For the Enzyme and NCI1 experiment, we set the walk length to be 6 in both version of the quantum network. The output neural net is a set2vec layer (for aggregation) followed by single layer. The feature and hidden layer dimensions are all set 64. In Mutag, the walk length is reduced to 4 and the layer size to 16. The GCN and DCNN are used as the input layer to a similar neural network i.e a set2vec layer followed by a hidden layer of size 64 (16 for Mutag).

**Regression** For QM7 we use quantum walk networks using a 4-step walk, followed by the set2vec layer with a hidden size of dimension 10. A similar setup is followed for DCNN and GCN models.

All models are trained with Adam optimizer with a learning rate of 1e-3.